Significant Variations of Radiosonde Ascent Rates

Observed Above a Severe Tornadic Thunderstorm

W.H. Blackmore

Upper Air Observations Program, Technical Report 2017-1

Office of Observations W/OBS33

NOAA National Weather Service Headquarters

May, 2017

INTRODUCTION

Lane, et al (2003) examined radiosonde data and showed that changes in the radiosonde ascent rate can be caused by gravity waves generated by nearby thunderstorms A preliminary report by Blackmore and Kardell (2012) examined more than a dozen cases of radiosonde ascent rates above 20 km where there were strong variations in ascent rate. Gravity waves induced by severe thunderstorms were suspected as a common cause for them.

Shortly after 00:00 UTC April 28, 2014, a severe thunderstorm with an EF-4 tornado struck central Arkansas (Buonanno, et al. 2014). Additional details on the storm are provided here:

http://www.srh.noaa.gov/lzk/?n=svr0414c.htm

http://www.spc.noaa.gov/exper/archive/event.php?date=20140427

The National Weather Service office in Little Rock, Arkansas, made three radiosonde observations prior to the April 28 severe weather event. From these soundings, radiosonde ascent rates and the location of the radiosonde before and during the severe weather event are analyzed in this study.

DATA ANALYSIS

Blackmore and Kardell (2012 and 2014) provide details on the characteristic of the balloons used for NWS soundings and the calculation of radiosonde ascent rates.

Table 1 shows the observation time, radiosonde release time, and observation termination (all balloon burst) height for three radiosonde soundings taken at the NWS office in Little Rock, AR.

Observation Time (UTC)	Radiosonde Release Time (UTC)	Observation Termination Height (meters)
18:00 April 27, 2014	17:10	33,046
21:00 April 27, 2014	20:31	33,585
00:00 April 28, 2014	23:02	30,735

Table 1: Radiosonde soundings taken at the Little Rock office.

Figures 1 through 3 show ascent rates from the three Little Rock soundings. Note the very erratic ascent rates in Figure 3, beginning near 20 km. The ascent rate was slightly negative (descending radiosonde) just above 22 km and exceeded 13 m/s near 32 km. The maximum echo top for the storm was less than 60,000 feet (18.3 km), so most of the oscillations seen are occurring in clear air well above the thunderstorm. Radar echo top imagery with the corresponding location of the radiosonde and its' height at the same time are shown in Figures 4 and 5. Figure 6 marks the radiosonde ascent rates at the time of the radar imagery shown in Figures 4 and 5.

In Figure 7, layers where updrafts (noted as "U") and downdrafts (as noted as "D") were occurring are labeled. For layer D2, the downdraft was so strong that the radiosonde stopped rising and descended for a brief period. The radiosonde temperature data is overlaid in Figure 7 and note the warming of the temperature during each occurrence of a downdraft. Likewise there is cooling of the temperature during an updraft. The warming and cooling temperatures are likely from adiabatic heating/cooling of the descending/ascending air mass. Figure 8 shows a Stuve Diagram for this sounding. Note the slopes of the temperature profile are closely parallel to the dry adiabatic lines (green lines). The severe thunderstorm in this case likely influenced the temperature profile well above the storm cloud tops.

Figures 9 and 10 show the locations of updrafts and downdrafts as noted in Figure 7 overlaid on Google Earth imagery. In Figure 10, a closer view is shown and the updrafts and downdrafts occurred in a cluster less than 4 km wide at the widest point over the town of Searcy, Arkansas. Winds aloft above 20 km were variable in direction with speeds 15 knots or slower so the radiosonde did not drift far.

SUMMARY

In this study, three radiosonde observations were taken about three hours apart before and during a significant severe weather event. Gravity waves were generated by the thunderstorms and propagated vertically in the stratosphere and well above the storm cloud tops. The radiosonde data were affected by these waves and showed abrupt changes in the rise rate of the radiosonde, as well as likely caused layers of adiabatic cooling and heating of the temperature data.

REFERENCES

Blackmore, W. H., and R. Kardell, 2012: Observations of significant variations in radiosonde ascent rates above 20 km. A preliminary report. NWS Headquarters Observing Systems Branch Special Studies, 55 pp.

Blackmore, W. H., and R. Kardell, 2014: Application of Radiosonde Ascent Rate Variations to Detect Atmospheric Turbulence Affecting Aircraft. NWA Journal of Operational Meteorology Vol. 2, No. 5 26, 51-58. [Available online at http://www.nwas.org/jom/articles/2014/2014-JOM5/2014-JOM5.pdf

Buonanno, C. C., and J. A. Lewis III, W. Gilmore, B. D. Smith, C. Rickard, C. Dalton, and S. Clarke, 2014: An Analysis of the 27 April 2014 Severe Weather event: The Mayflower-Vilonia-El Paso tornadic storm. 27th Conference on Severe Local Storms, American Meteorological Society, Madison, WI. Abstract available online: https://ams.confex.com/ams/27SLS/webprogram/Paper254466.html

Lane, T.P, and M.J.Reeder M.J., and F.M. Guest, 2003: Convectively generated gravity waves observed from radiosonde data taken during MCTEX. Q. J. R. Meteorol. Soc. (2003), 129, pp. 1731–1740

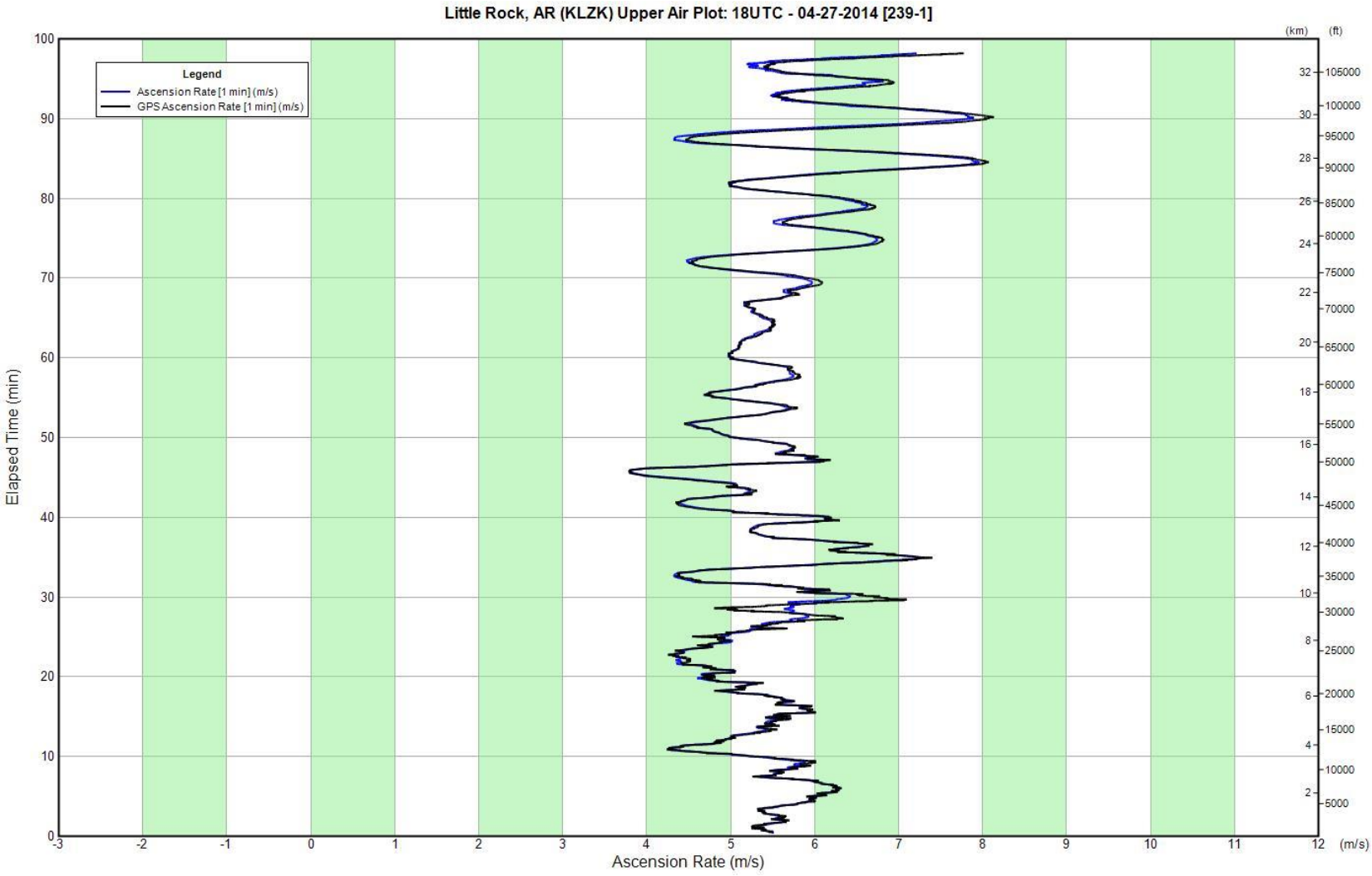

Figure 1. Little Rock 18:00 UTC, April 28, 2014 sounding of radiosonde ascent rate. X-axis is radiosonde ascent rate in m/s. Y-axis is elapsed time in minutes and height in feet and meters. Radiosonde ascent rate derived from the pressure sensor (blue) and GPS (black) are shown.

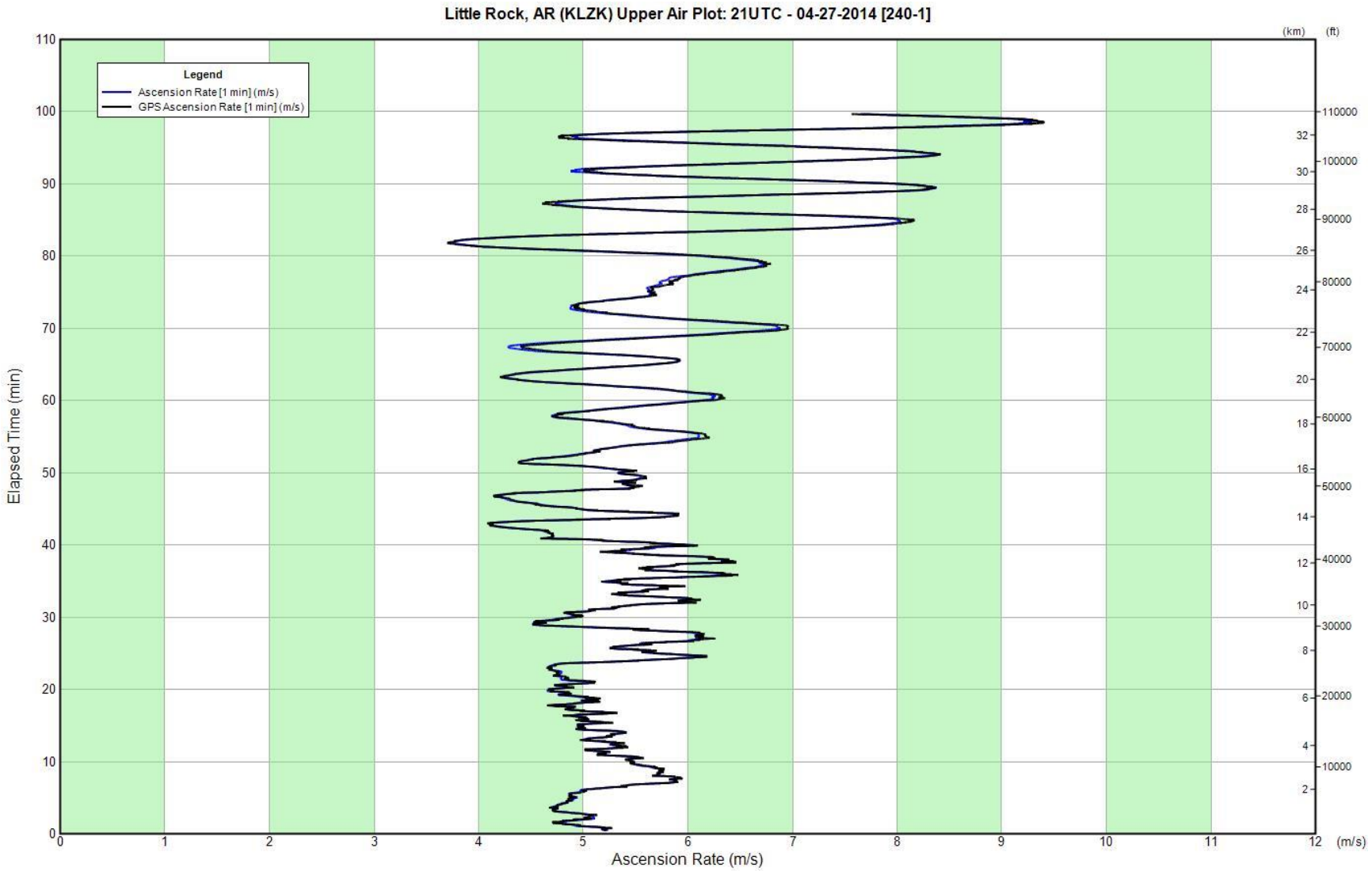

Figure 2. Little Rock 21:00 UTC, April 28, 2014 sounding of radiosonde ascent rate. X-axis is radiosonde ascent rate in m/s. Y-axis is elapsed time in minutes and height in feet and meters. . Radiosonde ascent rate derived from the pressure sensor (blue) and GPS (black) are shown.

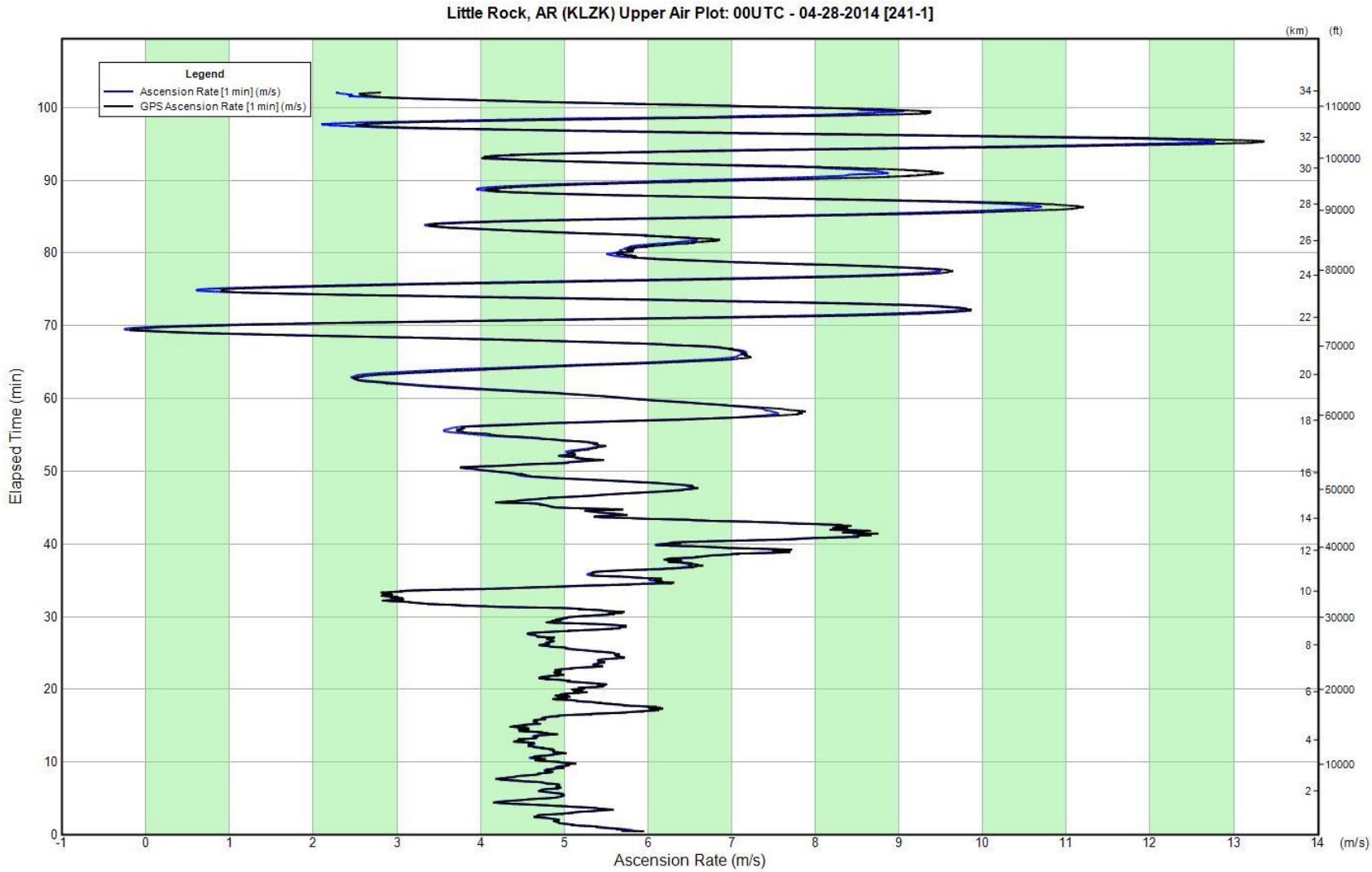

Figure 3. Little Rock 00:00 UTC, April 28, 2014 sounding of radiosonde ascent rate. X-axis is radiosonde ascent rate in m/s. Y-axis is elapsed time in minutes and height in feet and meters. Radiosonde ascent rate derived from the pressure sensor (blue) and GPS (black) are shown.

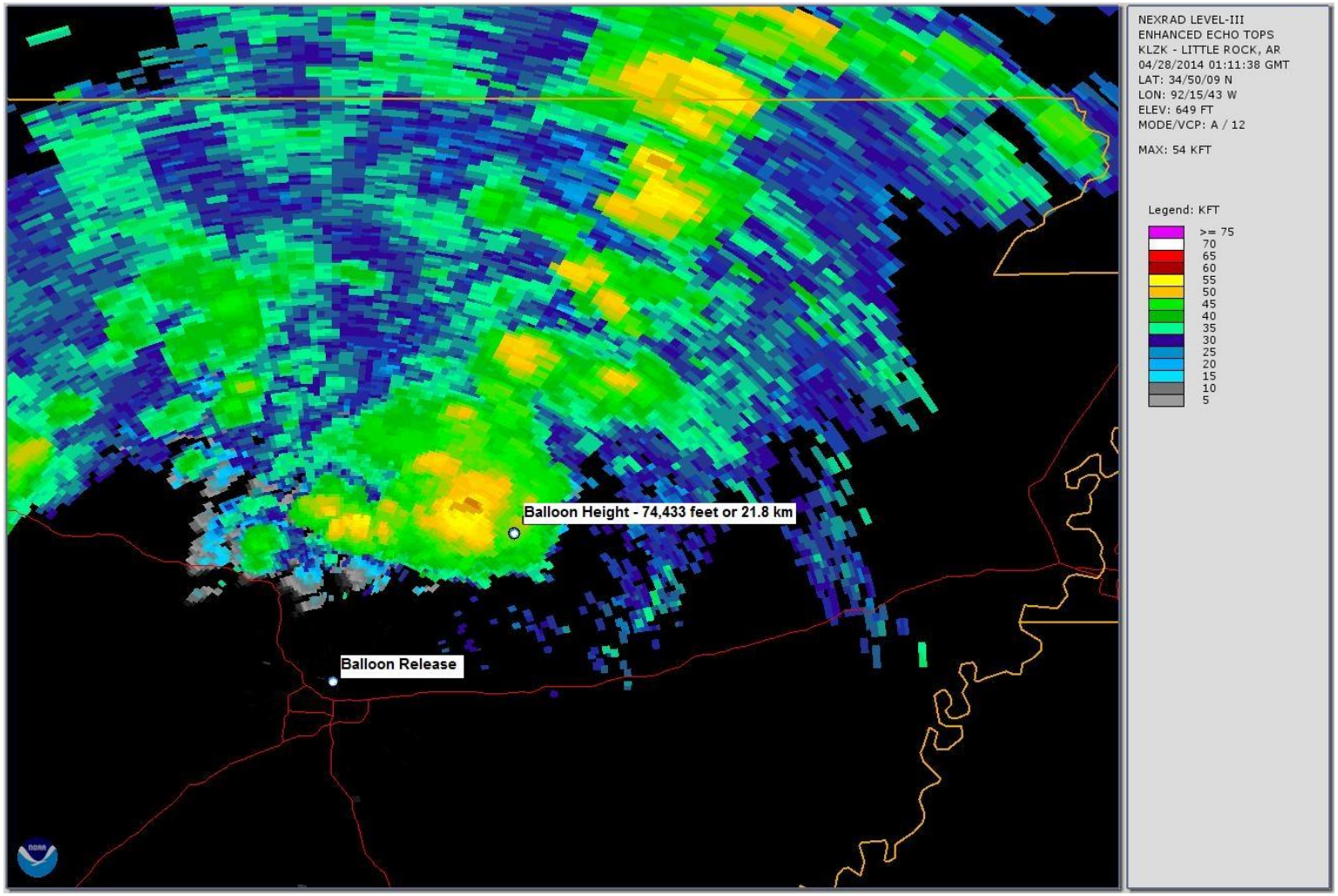

Figure 4. 01:11:38 UTC radar echo tops observed by the Little Rock radar. Balloon release location and height of the 00:00 UTC radiosonde observation at the time of the radar imagery are overlaid. Echo top heights are in feet (MSL).

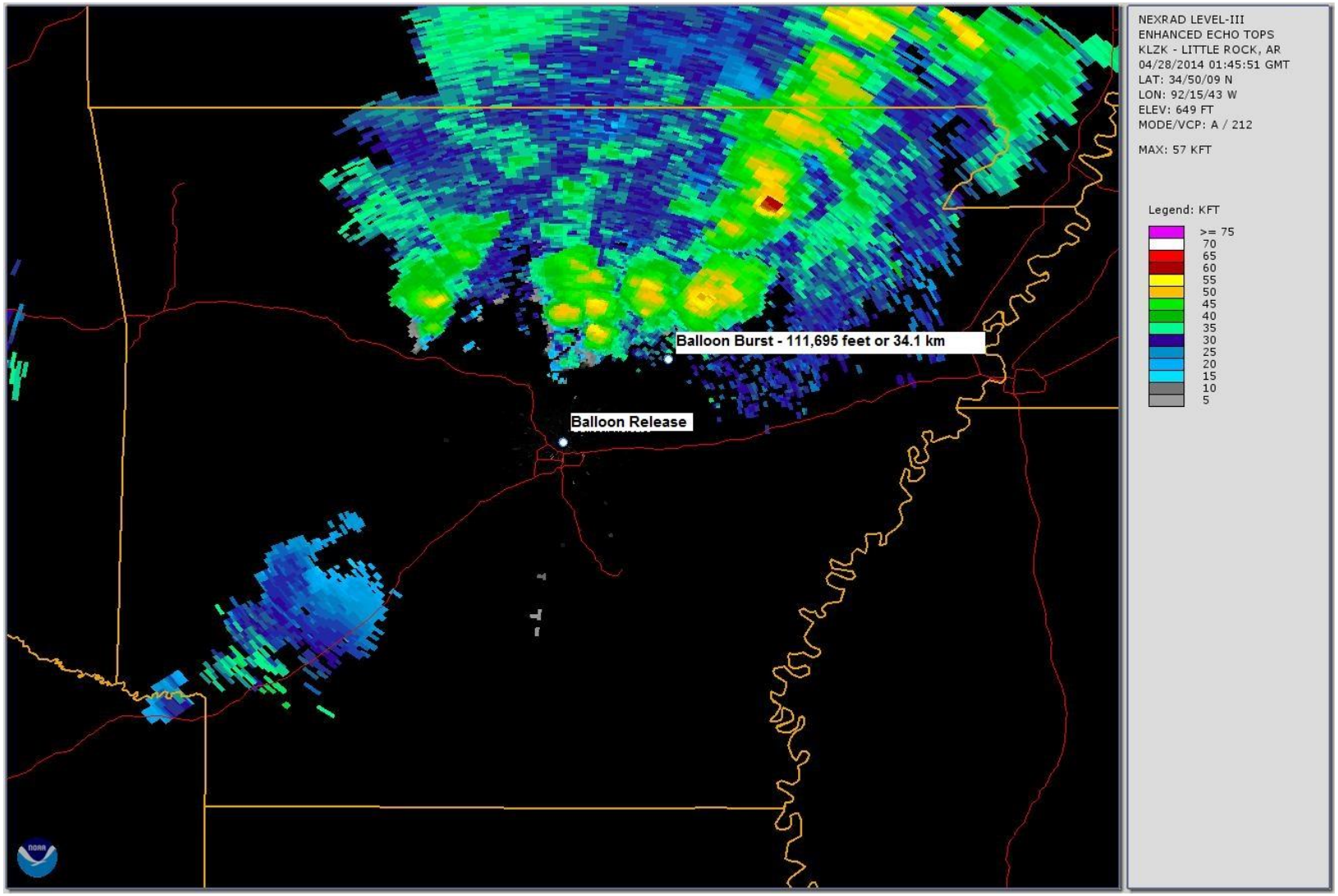

Figure 5. 01:45:51 UTC radar echo tops observed by the Little Rock radar. Balloon released location and height of the 00:00 UTC radiosonde observation at the time of the radar imagery are overlaid. Echo top heights are in feet (MSL).

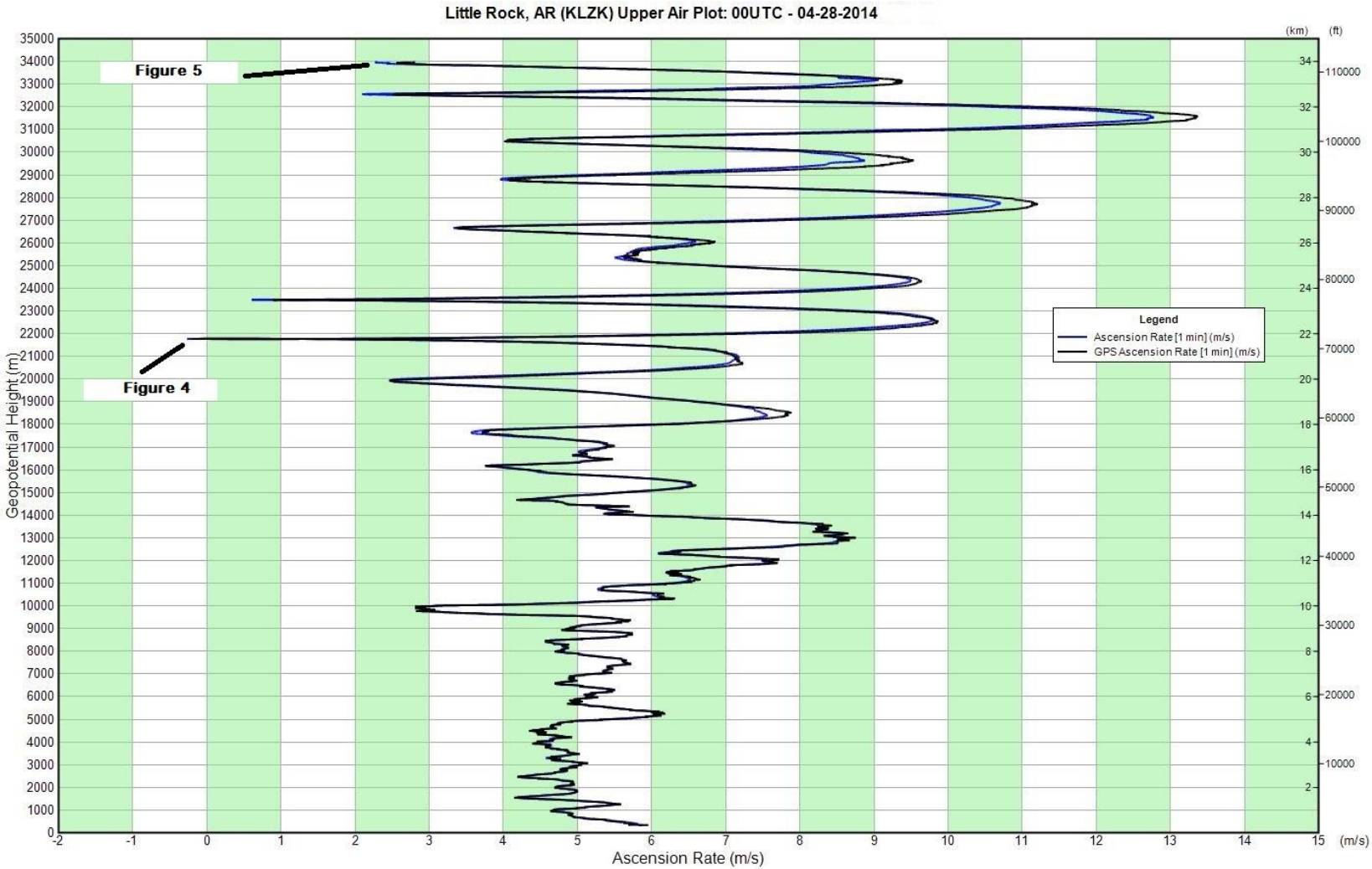

Figure 6. Same as Figure 3, but the height of the radiosonde for Figure 4 and Figure 5 are shown. Radiosonde ascent rate derived from the pressure sensor (blue) and GPS (black) are shown.

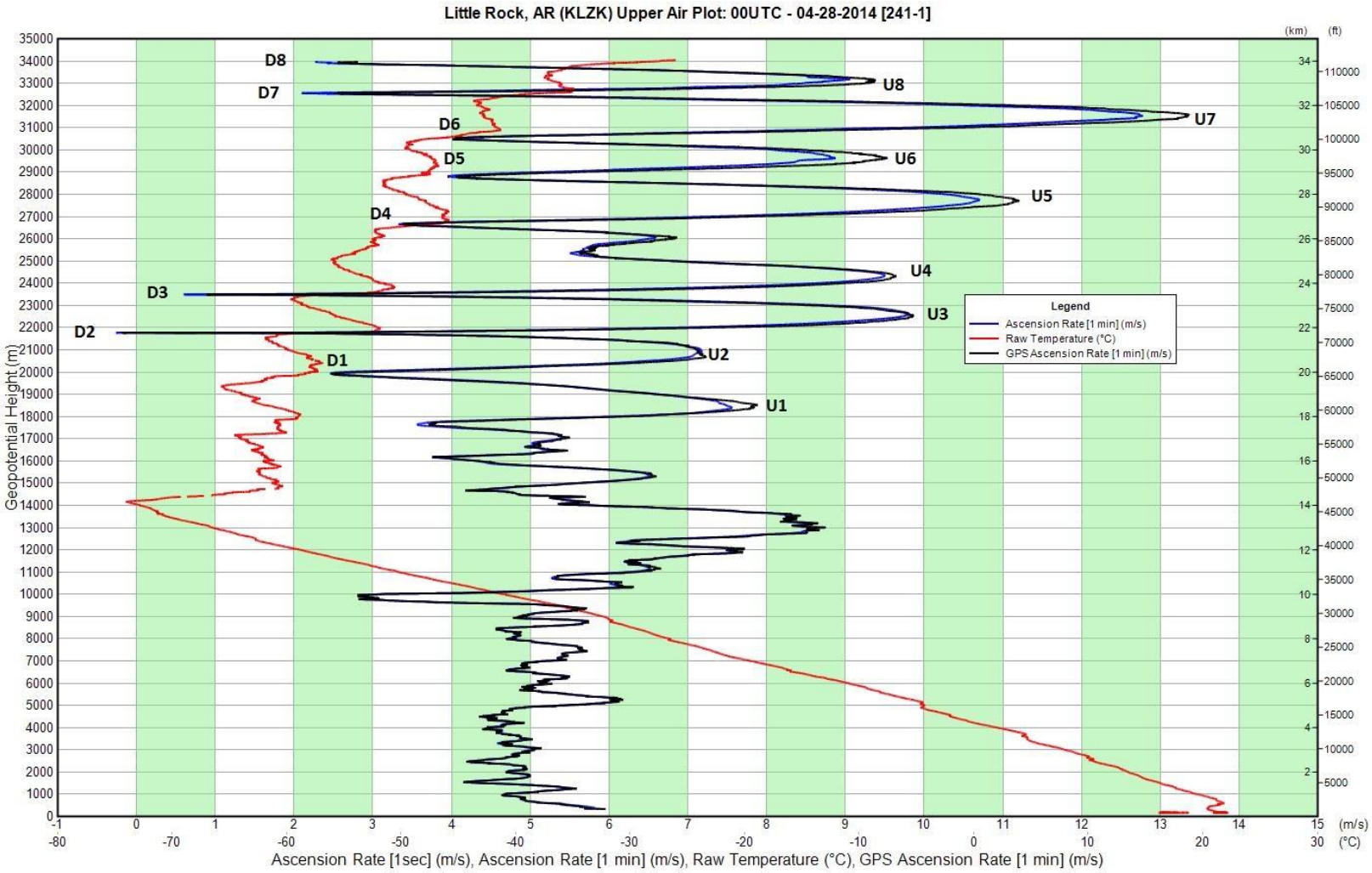

Figure 7. Same as Figure 3, but updrafts are marked as a “U” and downdrafts marked as a “D”. One-second raw temperature (deg. C) data are also plotted.

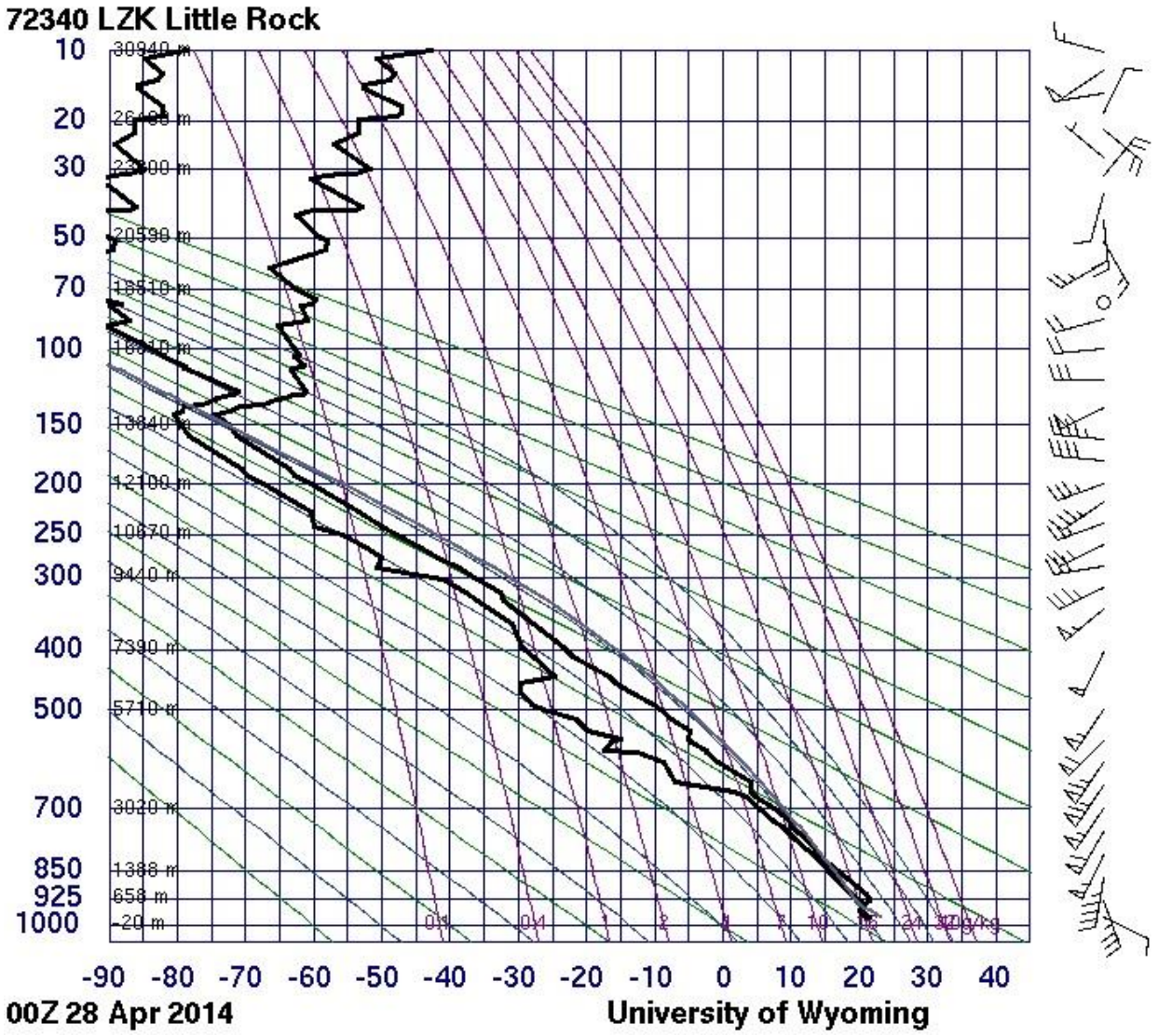

Figure 8. Stuve diagram to 10 hPa. (Plot Courtesy of the University of Wyoming)

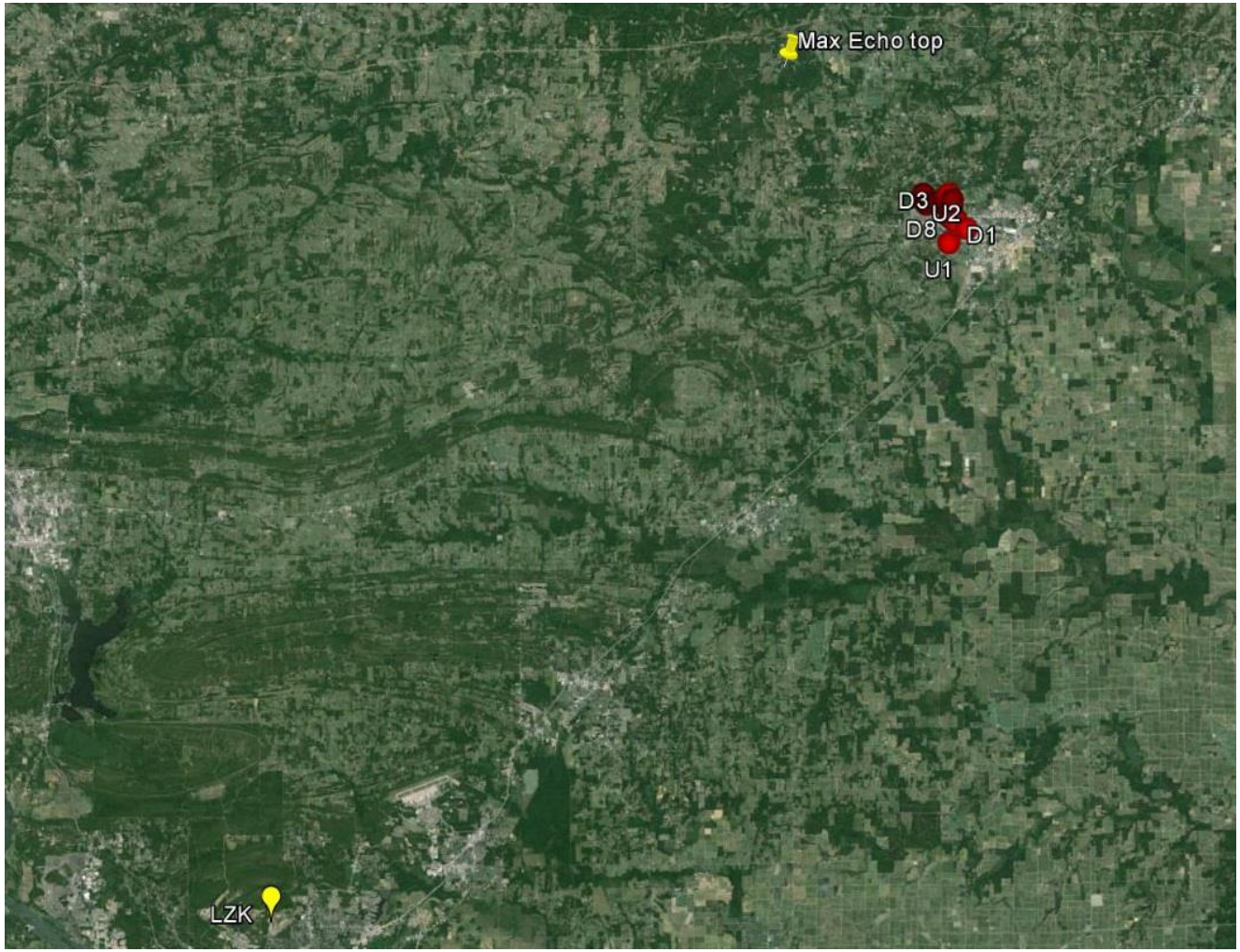

Figure 9: Google Earth photo showing the locations of the radiosonde release location (LZK), the cluster of updrafts and downdrafts from the Little Rock 00:00 UTC, April 28, 2014 sounding. Also shown is the location of maximum radar echo top. Distance of max echo top to cluster is about 15 km. The distance from LZK to cluster center is about 65 km.

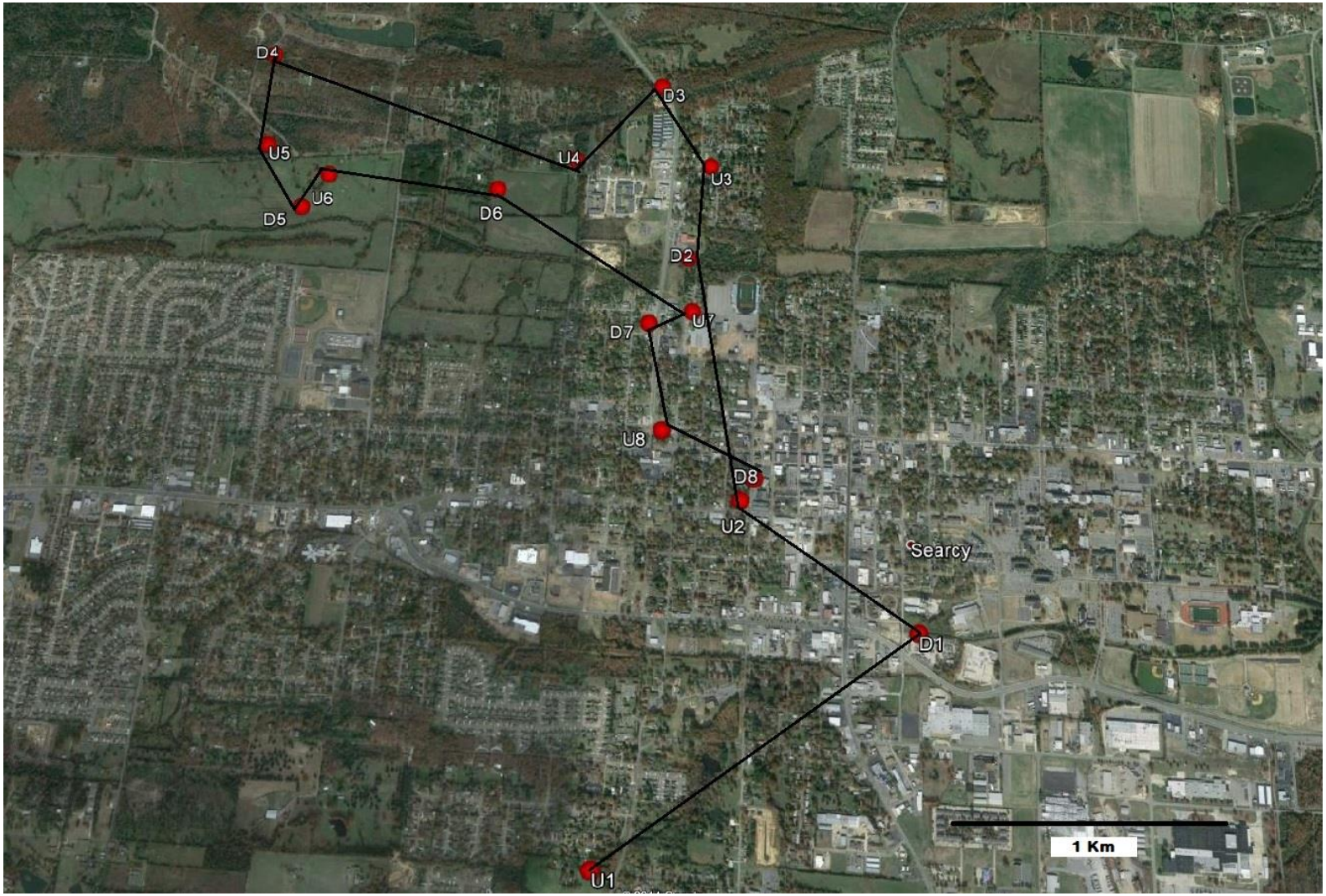

Figure 10. Close-up Google Earth photo of the locations of the “U” and “D” points shown in Figure 8. The distance from D1 to D4 is 3.75 km. The cluster occurred over the town of Searcy, Arkansas.